Absolute measurements of anomalous small-angle X-ray scattering intensity using glassy carbon at the Mg K absorption edge

Aoyama, Keita; Okuda, Hiroshi; Lin, Shan; Mase, Kazuhiko; Kitajima, Yoshinori; Tamenori, Yusuke

Japanese Journal of Applied Physics 61, 070915 (2022)

https://doi.org/10.35848/1347-4065/ac7a7e

Absolute measurements of anomalous small-angle X-ray scattering intensity using glassy carbon at the Mg K absorption edge

Keita Aoyama[1†], Hiroshi Okuda[1*], Shan Lin[1‡], Kazuhiko Mase[2], YOSHINORI Kitajima[2] and Yusuke Tamenori[3]

[1]*Department of Materials Science and Engineering, Kyoto University, Kyoto, Kyoto 606-8501, Japan.*

[2] *High Energy Accelerator Research Organization, Tsukuba, Ibaraki 305-0801, Japan*

3 Japan Synchrotron Radiation Research Institute, Spring8, Sayo, 679-5198, Japan.

E-mail: okuda.hiroshi.5a@kyoto-u.ac.jp

Absolute measurements of small-angle X-ray scattering (SAXS) intensities at the K absorption edge of Mg have been performed using glassy carbon as an intensity standard. Glassy carbon samples polished down to give appropriate transmission have been prepared as a secondary standard to be used at 1.3 keV. Al-Mg binary alloys were used to assess metastable phase boundary for the Al_3Mg metastable precipitation from the absolute scattering intensity. The assessed phase boundary agreed with the previous reports. Glassy carbon was concluded to be an appropriate candidate for an intensity standard sample for transmission measurements of SAXS in the tender X-ray regions.

† Present address：Rohm Corp. Ltd.， Kyoto、Japan.

‡ Present address: Institute of Metals Research, Chinese Academy of Sciences, Shenyang, Liaoning, People’s Republic of China.

Small angle X-ray scattering (SAXS) is widely used for structural analysis of phase separation occurring in nanoscopic scale[1-5]. It has been applied to investigate the phase decomposition processes of supersaturated solid solutions in Al alloys.[6-12] The SAXS method has advantage over microscopic approaches in several points. For example, acquired data reflect macroscopic average of nanostructures, and in-situ / nondestructive measurements are easily performed owing to better transmission and higher incident flux at synchrotron radiation facilities. Further, since the SAXS profile gives a Fourier transform of the electron density, the method is more easily applied to examine weak fluctuations without well-defined interfaces, like initial stage of spinodal decomposition[13-16], weak compositional and density fluctuation in disordered materials[17] or critical scattering[18]. However, since the origin of the scattering is the difference in the electron density, the method is hard to be applied to some of the materials of industrial importance. For example, the matrix and the precipitates in Al-Mg-Si alloys and Al-Mg alloys are composed of elements with neighboring atomic numbers, consequently quantitative analysis of such low-contrast structure is difficult.

Anomalous Small Angle X-ray Scattering (ASAXS) [19-23] is a useful method to evaluate the low-contrast precipitation structure[23] or the environmental nanostructures by calculating partial structure functions[19, 22, 23]. Therefore, ASAXS analysis might be a promising candidate for quantitative analysis of precipitation microstructures in Al-Mg-based alloys. The technical difficulties to perform ASAXS analysis for the alloy come from the fact that the absorption edges of the elements lie in the so-called tender X-rays region, at which the transmission through the materials, even through air and window materials, is very low and all the measurement systems need to be housed in vacuum.

In the present study, we designed a chamber housing all the optical components of the SAXS camera, i.e., a shutter, pinholes, intensity monitors, and a detector, with adjustable camera length. The camera length covers from 5 to 20 cm, corresponding to the camera length of approximately 50 cm to 2 m of the conventional SAXS at 12.4 keV. The camera chamber is schematically illustrated in Fig.1. The present chamber is a revised version of the one used in the previous work[24].

In the present work, the same detector, a phosphor plate coupled with fiber optics (FOT) and a CCD was directly mounted on a new chamber. In the previous work, we preformed ASAXS measurements of annealed Al-Mg alloys and MgO nano powders, and concluded that the relative contrast change agreed with the one expected from calculated anomalous

scattering factors[25, 26]. However, standard procedure of quantitative SAXS analysis requires that the intensity need to be expressed in absolute units, i.e., electron units per unit volume, for detailed analysis. For this purpose, we need an intensity standard sample.

For the intensity standard samples in hard X-ray regions, several materials such as water, polyethylene, glassy carbon, etc., have been reported[27-29]. In the present work, a standard sample needs to fulfill the following requirements.

1) The sample should be used in transmission mode, and stable enough against environmental and radiation damage expected for the use in the tender X-ray region under vacuum.

2) The sample can be easily polished for an optimal thickness for the wavelength of use, since the change in the transmission is relatively large in the tender X-rays region. It also means that the price and the availability need to be reasonable.

3) The sample gives strong scattering in the scattering vector range of interest.

4) The sample does not contain elements whose absorption edges exist within the energy range of interest.

From these requirements, glassy carbon samples supplied by Nilaco Co. Ltd. were used as secondary standard samples, with the glassy carbon sample supplied by Ilavsky et al.[29,30] as the primary standard to calibrate the second ones.

The experiment was conducted at BL13A of the Photon Factory of the High Energy Accelerator Research Organization (KEK) and the results were compared with those obtained at BL27SU of SPring8. An insertion device is used and a high vacuum path is provided downstream, allowing the use of a high intensity incident X-ray beam. The incident beam intensity was monitored by photoelectrons current at the upper stream Au mesh in the beamline, and the transmission intensity through the sample was measured by a photodiode in the SAXS chamber.

After background correction and normalization with respect to the incident flux, normalized SAXS intensity, I_{coh}, is given by;

$$I_{coh}(q) = \frac{1}{d}\left(\frac{I_{obs}(q)-I_{obsdark}(q)}{I_0 \cdot t \cdot T} - \frac{I_{blank}(q)-I_{blankdark}(q)}{I_{blank0} \cdot t_{blank}}\right) \qquad (1)$$

where I_{obs} and I_{blank} denote the intensity measured with and without the sample in the sample holder respectively. I_0 and I_{blank0} are the photon flux of the incident X-rays at the beam monitor, t and t_{blank} are the exposure time, I_{dark} is the intensity detected by the

CCD camera without incident light and d is the sample thickness.

To express the intensity $I_{coh}(q)$ in the absolute unit, a standard sample with known absolute intensity need to be measured at the same time. For this purpose, scattering intensities of a thin glassy carbon standard were measured at each measurement conditions. To prepare the secondary standard samples, glassy carbon discs with 50 mm diameter and 1mm thickness was purchased from Nilaco and used for raw material to polish down to an appropriate thickness[31]. The SAXS intensities of as-purchased samples were measured along with the primary standard glassy carbon sample (rot/sample number H8, hereafter denoted as H8) provided by Dr. Ilavsky, ANL[29] with absolute intensity data under the same measurement conditions. After measuring the specific density in the original disc form, the Nilaco glassy carbon samples, hereafter denoted as SD2, were cut and polished down to the thickness of about 20 μm, appropriate for the photon energy of the present work. The thickness of the secondary standards after polishing were calculated from the transmission of the sample and the evaluated specific density of the starting material and the attenuation constant[25)26)]. The measurements of the glassy carbons with 1mm thickness were carried out with hard X-rays of 8.26 keV or 12.4 keV at the beam-lines 6A and 10C of photon factory, and those for the thin secondary samples were performed at the beam-line 13A of Photon Factory and the beam-line 27XU of SPring-8. Figure 2 shows the SAXS intensities of the primary (H8) and the secondary (SD2) glassy carbon samples. SD2 samples were calibrated with the primary standard sample by measuring the both sample under the same conditions with hard X-rays. Then, a SD2 sample polished down to 20 μm for appropriate transmission at tender X-rays was measured at 1288 eV, and shown in the figure.

The absolute intensity of the secondary as-purchased sample was calibrated by the primary standard sample. The SAXS profiles of the secondary standard samples before and after polishing agreed with each other, while the SAXS profiles for H8 and Nilaco are slightly different, suggesting that both of the glassy carbon samples have similar characteristic void size and volume fraction with slightly different spatial arrangements of the voids. From the transmission at the four photon energies between 1302 eV and 1265 eV, the thickness of the secondary sample used in the present work was 20.39±0.05 μm. It is therefore concluded that polishing down the secondary standard sample is a reasonable approach to prepare a standard sample fit for an appropriate attenuation for the absolute measurements in the tender X-rays region.

To apply the absolute measurements to a low-contrast alloy systems, Al-Mg alloy samples used in the previous work on anomalous SAXS in relative scale[24] were chosen. The

compositions were Al-12.85 mass% Mg and Al-15.8 mass% Mg. The heat treatment conditions were artificial aging at 313 K for 1 week, followed by storage at room temperature for about 5 years. Under this artificial aging condition, the spherical G.P. zones are reported to reach metastable state and have weak anisotropic spatial arrangements with 4-fold symmetry when viewed from <100> incidence[24, 33, 34]. Measurements were performed at four energy levels below the K absorption edge of Mg, 1305.8 eV, i.e., 1265 eV, 1285 eV, 1298 eV, and 1302 eV, with the secondary standard sample. In general, measured SAXS intensities contain the scattering whose origin is other than the precipitates, e.g., surface oxides, oxide inclusions, and lattice defects such as dislocation cells and voids. These scattering components are the coherent scattering from the samples, and therefore are difficult to remove using background measurements. Such components were found to be relatively strong in the present measurements. However, considering that such scattering source generally do not contain the element chosen for the present anomalous effect, they are expected to give the scattering intensities independent of the photon energy. Therefore, we use the difference in the intensity measured at two energies, E and E', to extract the intensity component for E=1288 eV, 1298 eV and 1302 eV after subtracting that for E'=1265 eV, and (b) Al-12.85 mass% Mg and 15.8 mass% Mg for E=1288 eV after the subtraction. Figure 3(a) shows that the SAXS intensity is the same except the amplitude, reflecting the change in the anomalous scattering factor.

The integrated intensity in absolute units, Q_0, is related to the difference in the electron density between the matrix and the precipitate, $\Delta\rho$, and the volume fraction of the precipitates, V, for conventional (non-resonant) SAXS under two-phase model as;

$$Q_0 = \int_0^\infty I_{abs}(q) q^2 dq = 2\pi^2 \langle \Delta\rho^2 \rangle V(1-V) \ . \qquad (2)$$

Equation (2) is also expressed in terms of the mole fraction of Mg in the sample, m_A, and the miscibility gap composition for the matrix side, m_1, and the precipitate side, m_2, as given by Gerold et al. [7, 8]

$$\frac{Q_0(m_A,E)-Q_0(m_A,E')}{\sigma_e} = 2\pi^2 \frac{\left\{(\Delta f_1(E))^2-(\Delta f_1(E'))^2\right\}p}{{v_a}^2}(m_1-m_A)(m_A-m_2) \qquad (3)$$

where σ_e is the Thomson total cross section of electron, expressed as $\frac{8\pi}{3}{r_e}^2$ where r_e is the classical electron radius. v_a is the atomic volume in the matrix, and Δf_1 is the difference in the real part of the atomic scattering factors between Al and Mg[26]. $1-p$ is the degree of supersaturation. For the coarsening stage, p=1 and Q_0 is an invariant parameter for the SAXS determined by the phase diagram. The samples were in the

coarsening process as demonstrated in the previous work[24]. Then the miscibility gap at T=313 K, m_1 and m_2 are obtained from the measured integrated intensities for two independent m_A. The miscibility gap compositions were m_2=20.1±0.9 mol% at the precipitate side and m_1=13.0 ±0.3 mol% for the matrix side, respectively. The results are plotted in Fig. 4 with reported phase boundaries.

Use of glassy carbon as a machinable secondary standard material was demonstrated as a reasonable approach for absolute SAXS measurements in the tender X-rays region, and applied to microstructure analysis of Al-Mg binary alloys.

Normalization of ASAXS intensities for Al-Mg alloys into absolute intensity using a polished glassy carbon sample having appropriate thickness was made successfully at K absorption edge of Mg. Comparison with preceding works[34-39] on the estimation of the solubility limit using ultrasonic, thermal analysis, and electron microscopy, present results give good agreement for the experimental solubility limit on the matrix side and also reasonable agreement with the calculated phase boundary on the precipitate side.

Acknowledgments

Present work has been financially supported by the grant-in-aid for scientific research 25286085 and 18H05476 .and Light Metals Educational Foundation. Synchrotron radiation SAXS measurements have been approved by 2016G563, 2018G553 and 2020G637 of Photon Factory and 2016A1408, 2018B1205 of SPring8.

References

1) A. Guinier, and G. Fournet, *Small-angle scattering of X-rays* (Wiley, New York, 1955).
2) L.A.Feign, and D. I. Svergun. *Structure Analysis by Small-Angle X-ray and Neutron Scattering*. (Springer, New York, 1987).
3) O Porod and O. Glatter eds., *Small-Angle X-ray Scattering* (Academic Press, New York, 1983).
4) V. Gerold, Phys. Status Solidi b, 37 (1961). [in German].
5) G. Kostorz, *Physical Metallurgy*, ed. R. W. Cahn and P. Haasen (North Holland Amsterdam, 1996) 4th ed. Chap. 12.
6) A. Guinier, Nature, **142**, 567 (1938).
7) R. Bauer and V. Gerold Acta Metall., **10,** 637 (1962).
8) V. Gerold, J.E. Epperson and G. Kostorz, J. Appl. Crystallogr. **10**, 28 (1977).

9) K. Osamura, and Y. Murakami, J. Jpn. Inst. Metals. **43**, 537 (1979). [in Japanese]
10) S. Komura, K. Osamura, H. Fujii, and T. Takeda Phys. Rev. **B30**, 2944 (1984).
11) H. Okuda, I. Tanaka, T. Matoba, K.Osamura and Y.Amemiya ; Scr. Mater, **37**, 1739(1997).
12) P. Donnadieu, Y. Shao, F.De Geuser, G.A.Botton, S .Lazar, M. Cheynet, M.de Boissieu, and A. Deschamps, Acta Mater. **59**, 462 (2011).
13) K. B. Rundman and J.E. Hilliard ; Acta Metall., **15**, 1025 (1967) .
14) R.Acuna and A.Bonfiglioli; Acta Metall. **22**, 399 (1974).
15) G.Laslaz, G.Kostroz, M.Roth, P. Guyot and R.J.Stuwert, Phys. Stat. Sol. **41**, 577 (1977).
16) J.S.Langer, Bar-on, Miller Phys. Rev. **11A**, 1417 (1975)
17) A. B. Bhatia and D. E. Thornton.Phys. Rev. B **2**, 3004 (1970).
18) D.Schwahn and W. Schmatz, Acta Metall. **26,** 1571 (1978)
19) .O.Lyon, *Methods in the Determination of Partial Structure Factors*, Ed.JBSuck et al., Proc. ILL/ESRF Workshop,(World Scientific, Singapore 1993) p.142.
20) A. Naudon. *Modern Aspects of Small-Angle Scattering*, ed. H. Brumberger (Plenum,NewYork,1992) p.203.
21) H. B. Stuhrmann, J. Appl. Crystallogr. **40**, s23 (2007).
22) O. Lyon, J.P. Simon Phys. Rev. **B35**5164,(1987).
23) A.Hoell, F.Talchev, S. Haas, J. Haug, P. Boesecke, J. Appl. Crystallogr. **42**, 323 (2009).
24) H. Okuda, R. Sakohata, S. Lin, Y. Kitajima, and Y. Tamenori, Appl. Phys. Express, **12**, 075503 (2019).
25) D. T. Cromer and F. Liberman, J. Chem. Phys. 53, 1891 (1970).
26) https://physics.nist.gov/PhysRefData/FFast/html/form.html.
27) O.Kratky, I.Pilz, P.J.Schmitz, J. Colloid Interface. Sci. **21**, 24 (1966).
28) C.A.Dress, K.S. Jack, A.P.Parker J.Appl. Cryst. **39,** 32 (2006).
29) A. J. Allen, F. Zhang, R. Joseph Kline, W. F. Guthrie, and J. Ilavsky, J. Appl. Crystallogr. **50**, 462 (2017).
30) F.Zhan, Jan Ilavsky, G. G. Long, J P.G. Quintana, A. J. Allen, and P R. Jemian; Metall. Mater. Trans. **41**, 1151 (2009).
31) H.Okuda, T.Yamamoto, K. Takeshita, M.Hirai, K. Senoo, H.Ogawa, Y.Kitajima, Jpn. J. Appl.Phys. **53** ,05FH02 (2014).
32) A.Dauger, M.Fumeron, J.P.Guillot M.Roth J.Appl.Cryst. **12**, 429 (1979).
33) M. Hennion, D.Ronzaud, P.Guyot, Acta Metall., **30**, 599 (1982).
34) M.J.Starink and A.M.Zahra, Phil. Mag. **76A**, 701 (1997).
35) C. Gault, A. Dauger and P. Boch: Acta Metall., **28** ,51 (1980).

36) M. J. Starink and A.-M. Zahra: Acta Mater., **46** , 3381 (1998).

37) T. Sato, T. Takahashi, H. Iizumi, and K. Doi ; J. JILM, 110 (1984).

38) M. V. Rooyen, J. A. Sinte Maartensduk and E. J. Mittemeijer: Metall. Trans. A, **19** , 2433 (1988).

39) S.Kogo, H.Iwaoka, and S.Hirosawa Jpn.J.LightMetals,**67**,173 (12017).[in Japanese]

Figure Captions

Fig. 1. Schematic illustration of SAXS camera chamber used in the present work.

Fig. 2. SAXS intensities of two glassy carbon samples, the primary one (H8) with absolute intensity, and the other one purchased from Nilaco (SD2) as a secondary standard sample, whose absolute intensity was calibrated by the primary sample.
Conversion constant to absolute intensity were calculated by fitting the measured intensity between 0.6nm^{-1} and 1.0nm^{-1}

Fig. 3. Difference in absolute scattering intensities between (a) 1265 eV and 1288, 1298, 1302 eV for Al-12.85 mass % Mg, and (b) between 1265 eV and 1288 eV for Al-12.85 mass% Mg and Al-15.8 mass % Mg.

Fig. 4. Miscibility gap assessed from the present data, plotted with the reported solubility limit for the matrix side. The phase boundary proposed using thermodynamical calculations by Kogo et al.[39] is also shown by solid lines.

.

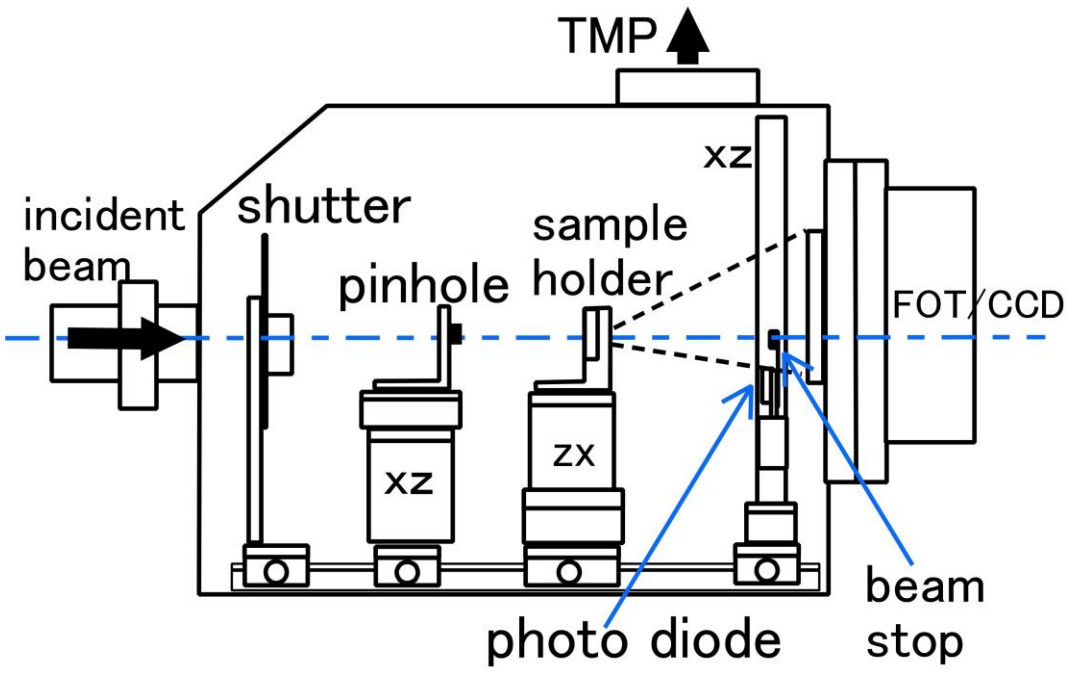

Fig.1. Schematic illustration of the SAXS chamber used in the present work.

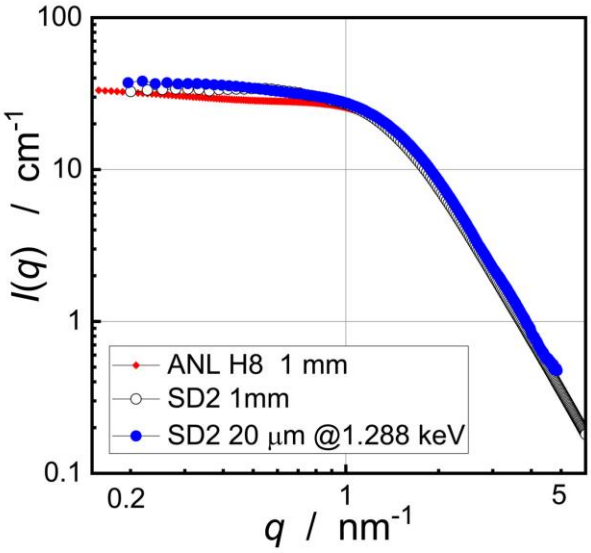

Fig.2 . SAXS intensities of two glassy carbon samples, the primary one (H8)with absolute intensity, and the other one purchased from Nilaco (SD2) as a secondary standard sample, whose absolute intensity was calibrated by the primary sample.
Conversion constant to absolute intensity were calculated by fitting the measured intensity between 0.6nm^{-1} and 1.0nm^{-1}

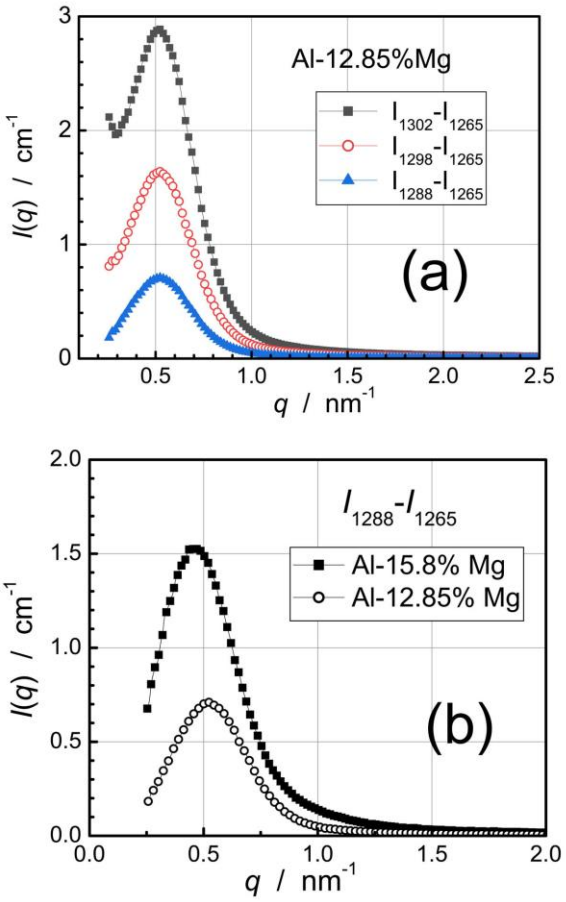

Fig.3. Difference in absolute scattering intensities (a) between 1265 eV and 1288, 1298, 1302 eV for Al-12.85 mass% Mg and (b) between 1265 eV and 1288 eV for Al-12.85 mass% Mg and Al-15.8 mass % Mg.

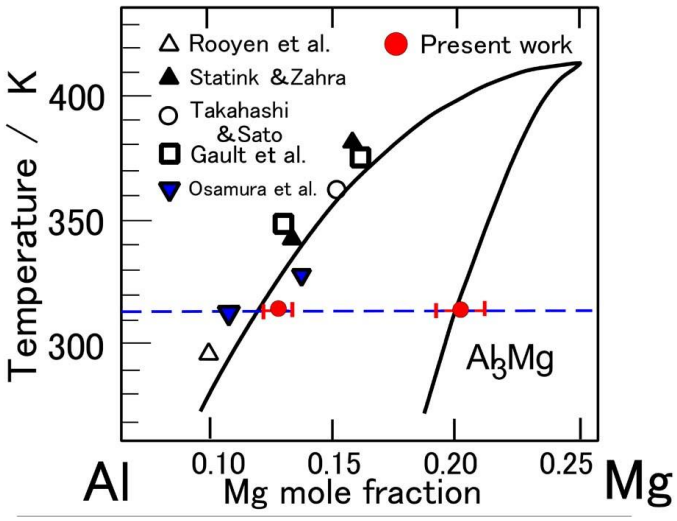

Fig.4. Miscibility gap assessed from the present data, plotted with the reported solubility limit for the matrix side. The phase boundary proposed using thermodynamical calculations by Kogo et al.[39] is also shown by solid lines.